Soft Matter

Cartilage Extracellular Matrix Polymers: Hierarchical Structure, Osmotic Properties, and Function

Journal:	*Soft Matter*
Manuscript ID	SM-ART-05-2024-000617.R1
Article Type:	Paper
Date Submitted by the Author:	08-Jul-2024
Complete List of Authors:	Horkay, Ferenc; National Institute of Child Health and Human Development, Section on Quantitative Imaging and Tissue Sciences Basser, Peter; National Institute of Child Health and Human Development Geissler, Erik; Université Grenoble Alpes

Data Availability Statement: The data that support the findings of this study are available from the corresponding author upon reasonable request.

Cartilage Extracellular Matrix Polymers: Hierarchical Structure, Osmotic Properties, and Function

Ferenc Horkay,[*1] Peter J. Basser,[1] and Erik Geissler[2]

[1] Section on Quantitative Imaging and Tissue Sciences, *Eunice Kennedy Shriver* National Institute of Child Health and Human Development, National Institutes of Health, 13 South Drive, Bethesda, MD 20892, USA. E-mail: horkayf@mail.nih.gov

[2] Laboratoire Interdisciplinaire de Physique (LIPhy), Université Grenoble Alpes and CNRS, F-38000 Grenoble, France

Abstract

Proteoglycans are hierarchically organized structures that play an important role in the hydration and the compression resistance of cartilage matrix. In this study, the static and dynamic properties relevant to the biomechanical function of cartilage are determined at different levels of the hierarchical structure, using complementary osmotic pressure, neutron scattering (SANS) and light scattering (DLS) measurements. In cartilage proteoglycans (PGs), two levels of bottlebrush structures can be distinguished: the aggrecan monomer, which consists of a core protein to which are tethered charged glycosaminoglycan (GAG) chains, and complexes formed of the aggrecan monomers attached around a linear hyaluronic acid backbone. The principal component of GAG, chondroitin sulfate (CS), is used as a baseline in this comparison.

The osmotic modulus, measured as a function of the proteoglycan concentration, follows the order CS < aggrecan < aggrecan-HA complex. This order underlines the benefit of the increasing complexity at each level of the molecular architecture. The hierarchical bottlebrush configuration, which prevents interpenetration among the bristles of the aggrecan monomers, enhances both the mechanical properties and the osmotic resistance. The osmotic pressure of the collagen solution is notably smaller than in the proteoglycan systems. This is consistent with its known primary role to provide tensile strength to the cartilage and to confine the aggrecan-HA complexes, as opposed to load bearing.

The collective diffusion coefficient D governs the rate of recovery of biological tissue after compressive load. In CS solutions the diffusion process is fast, $D \approx 3\ 10^{-6}$ cm^2/s at concentrations comparable with that of the GAG chains inside the aggrecan molecule. In CS solutions D is a weakly decreasing function of calcium ion concentration, while in aggrecan and its complexes with HA, the relaxation rate is insensitive to the presence of calcium.

Keywords: aggrecan, cartilage, chondroitin sulfate, osmotic modulus, collective diffusion coefficient

Introduction

Cartilage is a complex composite tissue consisting of fluid components (water and electrolytes) and a gel-like matrix containing chondrocytes, collagen fibrils, proteoglycans, *etc*.[1,2] In healthy cartilage, collagen (primarily type II) amounts to about 15% - 20% and proteoglycans 4 - 7% of the wet weight. The role of the collagen is to provide a resilient mesh in which the highly charged proteoglycans and their assemblies exert an osmotic force, counterbalanced by the elastic tension of the collagen fibers.[8] The high swelling pressure of the proteoglycans keeps the collagen network inflated, thus resisting deswelling under external load.

The most abundant proteoglycan in cartilage is the highly charged bottlebrush shaped molecule aggrecan.[3-6] It is composed of an extended protein core (approximate length 3000 Å) to which are attached about a hundred glucosaminoglycan (GAG) chains (chondroitin sulfate and keratin sulfate blocks) of length 200 - 500 Å. These act as bristles oriented randomly around the protein core, at intervals of 20 - 50 Å along its length. The distance between charges on the bristles ranges between 10 Å and 15 Å. As the length of the GAG chains is only two or three times greater than their persistence length, they impart stiffness to the overall aggrecan bottlebrush.

In cartilage, the aggrecan molecules form complexes by binding to long hyaluronic acid (HA) chains,[7] creating a secondary bottlebrush architecture of length several micrometers and radius 0.3 - 0.4 μm. *In vivo*, the aggrecan-HA bond is stabilized by link protein. The aggrecan-HA complexes enmeshed in the collagen matrix provide compressive resistance under external load. In a healthy individual, these complex load-bearing structures function in an almost friction-free manner throughout his entire life span. With age and disease, however, both the concentration

and composition of the proteoglycans are altered, and the large-scale structure degrades. Failure of joints leads to osteoarthritis, which ranks among the costliest health care challenges facing the developed world. To understand the pathogenesis of cartilage degeneration and to develop therapeutic strategies for its treatment requires knowledge of the physico-chemical interactions among the constituents of the cartilage extracellular matrix. In regenerative medicine, such knowledge is also essential to design improved implants that are tailored to match simultaneously the mechanical properties and biochemical composition of the replacement tissue.

To elucidate the relationship between structure and molecular function, the morphology, biochemical and mechanical properties of cartilage, as well as its main components, have been studied by many research groups. In his classical work, Ogston showed that the charged proteoglycans produce a high swelling pressure that keeps the cartilage inflated.[8] Maroudas attributed the increased hydration of osteoarthritic cartilage, compared with normal cartilage, to the weakening of the collagen network, which allows the tissue to swell, even with reduced glycosaminoglycan content.[9-11] Osmotic stress measurements by Basser et al.[12] on both healthy and osteoarthritic human cartilage samples showed that the collagen network acts to restrain cartilage hydration, and its loss in osteoarthritic cartilage reduces both the concentration of the proteoglycan and its osmotic pressure are severely diminished.

At the molecular level, a variety of techniques have been employed, e.g., NMR, small angle X-ray scattering, Fourier Transform Infrared Imaging (FTIRI) and Raman spectroscopy.[13-30] Solution NMR and high resolution magic angle spinning methods have revealed that the GAG chains in cartilage display large amplitude motions, similar to the free solution state. Solid state NMR spectroscopy investigations of the degree of hydration of collagen fibers indicate that the fibers are in a partially deswollen state.[21,32] The nanomechanical properties of proteoglycans, particularly of aggrecan, and their dependence on electrostatic interactions under different ionic conditions, have been extensively studied by Grodzinsky *et al*.[33,34] Combining high-resolution imaging with atomic force microscopy and mechanical measurements, these authors were able to quantify the effect of ionic strength on the forces acting between proteoglycan components and to interpret the results in the framework of poroelastic and viscoelastic models.

In previous studies, little attention has been paid to the thermodynamic properties of proteoglycans and their assemblies within the collagen matrix. In particular, neither the static nor the dynamic osmotic properties of these systems has been systematically investigated. Such

knowledge is needed to understand the underlying principles that govern the biomechanical performance of cartilage at each hierarchical level. Molecular dynamics simulations have shown that tethered aggrecan molecules exhibit strong mutual repulsion and interpenetrate to a very limited extent when forced together.[35-38] These calculations also showed that in the physiological pH range the aggrecan molecules are separated but that interpenetration increases at high concentrations of monovalent salt.[39] Recent experimental studies on aggrecan solutions, made by small angle neutron, X-ray and light scattering, confirmed the absence of significant penetration among the aggrecan bottlebrushes, and also revealed that both the structure and dynamics of aggrecan assemblies are largely insensitive to ionic strength, even in the presence of higher valence counter-ions. Aggrecan molecules and their complexes behave like microgels, i.e., under external loading and unloading they release and re-absorb fluid rapidly and reversibly.[35,36,40-42]

In this work we investigate the structure and dynamics of the main cartilage polymers at their different hierarchical levels of organization to analyze how they contribute to cartilage's biomechanical properties. The bristles in aggrecan are composed of linear GAG chains, chondroitin sulfate (CS) and keratin sulfate, tethered along the extended central protein core. Since CS is the predominant GAG, in the present study we use it as a model of the building block of the aggrecan bottlebrush.

The major function of cartilage is its load bearing resistance. We compare the osmotic pressure and osmotic modulus of the principal components, CS, aggrecan, aggrecan-HA complex and collagen. The spatial arrangement of these molecules at different levels of crowding is studied by small angle neutron scattering (SANS). Compressive loading and unloading are accompanied by changes in the volume of the tissue, i.e., changes in concentration. The response rate to volume change, due either to external loading or to changes in the ionic composition, is measured by the collective diffusion coefficient D of the water molecules and ions. D governs the efficiency of cushioning by the cartilage between bone ends. We compare the relaxation properties of the different components over a wide range of length scales using dynamic light scattering (DLS) and neutron spin echo (NSE) techniques. In cartilage, proteoglycans are confined in the collagen matrix. Although the principal role of the matrix is to immobilize the aggrecan-HA assemblies and to provide tensile stability to the cartilage, previous findings have indicated that the osmotic contribution of collagen to cartilage biomechanics is not negligible.[9-12] To estimate its order of magnitude, we determine this term both by DLS and by osmotic pressure measurements. Another

important function of cartilage is bone mineralization through accumulation of calcium ions, which therefore requires structural stability in the presence of this ion. We measure the effect of calcium ions on the osmotic pressure and on the collective diffusion coefficient for both CS and aggrecan solutions.

This multiscale approach can contribute to understanding the physico-chemical properties governing interactions among the macromolecular constituents of cartilage extracellular matrix, and lead to development of better biomechanical models and to improvement of design principles in tissue engineering of cartilage.[43,44]

Experimental Section

Materials and Methods

Sample Preparation

Aggrecan (bovine articular cartilage, Sigma) solutions were prepared in 100 mM NaCl. The concentration of the aggrecan was varied in the range $0.0002 \leq c \leq 0.05$ g/cm^3. A solution of aggrecan at $c = 0.0003$ g/cm^3 was also prepared in which the ratio of aggrecan to HA (Sigma, $M_w = 1.2\ 10^6$) was set equal to 100. To avoid the complexities of ternary polymer solutions, link protein, the role of which is that of a stabilizer of the aggrecan-HA complex,[9] was not included. The ionic strength and pH (= 7) were identical in all samples.

Collagen (from chicken sternal cartilage, Sigma-Aldrich) was first dissolved in acetic acid then neutralized by adding 2M Tris/HCl. The concentrations of the final solutions were in the range $0.003 \leq c \leq 0.1$ g/cm^3. The ionic strength and pH (= 7) were identical in all samples.

Chondroitin sulfate (Sigma-Aldrich) solutions were prepared with concentrations ranging between 1% and 20% w/w. Concentrations of added sodium chloride (NaCl) and calcium chloride ($CaCl_2$) were varied between 0 and 500 mM and 0 and 200 mM respectively. DLS measurements were made on CS solutions containing 100 mM NaCl, with concentrations of $CaCl_2$ between 0 and 200 mM.

In all samples the pH was 7, where CS is fully dissociated. The samples were allowed to homogenize for 2-3 days. All measurements were made at 25.0 °C ± 0.1 °C.

Osmotic Stress Measurements

The osmotic pressure of the aggrecan and collagen solutions was measured as a function of the polymer concentration by bringing them to equilibrium with polyvinyl alcohol (PVA) gels of known swelling pressure.[45-47] The dependence of the swelling pressure of the PVA gels on the PVA concentration was determined separately by equilibrating them with poly(vinyl pyrrolidone) (PVP) solutions of known osmotic pressure.[48] In this experiment the PVA gels were separated from the PVP solution by a semipermeable membrane. The PVP concentration was varied in the concentration range 1% w/w-< c < 20% w/w).

We used the calibrated PVA gels to measure the osmotic pressure of aggrecan and collagen solutions. The length of the PVA gel filaments was measured by optical microscopy after attaining equilibrium (ca. 24 h). The large size of the aggrecan and collagen molecules prevented them from penetrating into the swollen gel. The polymer concentrations were determined after equilibration gravimetrically. The reproducibility of the osmotic stress measurements was within 5%.

Small Angle Neutron Scattering Measurements

The SANS measurements[49,50] were made on the NG3 instrument at NIST, Gaithersburg, MD. Solutions were placed in sample cells of 1 mm optical path equipped with quartz windows. The wavelength of the incident radiation was $\lambda = 8$ Å, with wavelength spread $\Delta\lambda/\lambda = 0.10$. The transfer wave vector range explored was 2.8×10^{-3} Å^{-1} < q < 0.3 Å^{-1}, where $q = \frac{4\pi n}{\lambda}\sin(\theta/2)$, θ being the scattering angle and n the refractive index of the medium (in SANS experiments, n is close to unity). After azimuthal averaging, the spectra were corrected for detector response and cell window scattering.[51] The incoherent background, essentially due to protons in the sample, was subtracted following the procedure described previously.[52] Normalization was carried out using standard NIST samples.

Neutron Spin Echo (NSE)

The NSE measurements were made on the IN15 instrument at the Institut Laue Langevin, Grenoble, with $\lambda = 11$ and 15 Å. The length scales explored in the NSE measurements cover the range 30 Å > $1/q$ > 9 Å. These measurements explored time delays extending from 0 to 170 ns.

Light scattering

SLS and DLS measurements were performed in the angular range 20° to 150° with accumulation times of 200 s, using an ALV DLS/SLS 5022F goniometer and a 22 mW HeNe laser. The DLS field correlation functions $g(\tau)$ are derived from the Siegert relation

$$G(\tau) = 1 + \beta \left| g(\tau) \right|^2 \quad (1)$$

where $G(\tau)$ is the normalized intensity correlation function and $\beta = 0.98$ is the optical coherence factor of the instrument.

Semi-dilute polymer solutions frequently exhibit two main relaxation modes,[53,54] giving for $g(\tau)$

$$g(\tau) = a\exp(-\Gamma \tau) + (1-a)\exp\{-(\Gamma_s \tau)^{\mu}\} \quad (2)$$

where Γ and Γ_s are the fast and slow relaxation rates respectively. The fast relaxation rate Γ is diffusive, i.e.,

$$\Gamma = Dq^2 \quad (3)$$

where D is the collective diffusion coefficient describing the decay of the thermodynamic concentration fluctuations.[55]

The slow mode Γ_s in eq 2 arises from the presence of large, quasi-static domains. Such domains are common in associating polymer solutions and in many cases are so large that only internal modes are detected. This feature is often characterized by a relaxation rate that varies as q^3, and a decay mode that is similar to the second term in eq 2 in which the exponent $\mu \approx 2/3$. Owing to the large size of these domains, their contribution to the osmotic properties of the solution is negligible.

The intensity of the light scattered by the osmotic fluctuations, which is defined by $a_f\langle I(t)\rangle$, where $\langle I(t)\rangle$ is the time average of the total intensity scattered by the sample, is inversely proportional to the osmotic compression modulus $\kappa = c\partial\Pi/\partial c$, where Π is the osmotic pressure. Thus

$$a \langle I(t) \rangle = K k_B T c^2 / \kappa \quad (4)$$

where $K = [2\pi n_0 (dn/dc)/\lambda^2]^2$ is the optical contrast factor between the polymer and solvent. Here n_0 is the refractive index of the solution, λ the wavelength of the light and (dn/dc) is the refractive index increment. Since the value of (dn/dc) is known, both κ and Π can be estimated from eq. 4.

Results and Discussion

As noted above, cartilage is a complex tissue composed of several components that interact with each other and contribute differently to its biomechanical properties. Scheme 1 shows the polymer building blocks of cartilage. In Scheme 2 are shown the structural organization of of the main components.

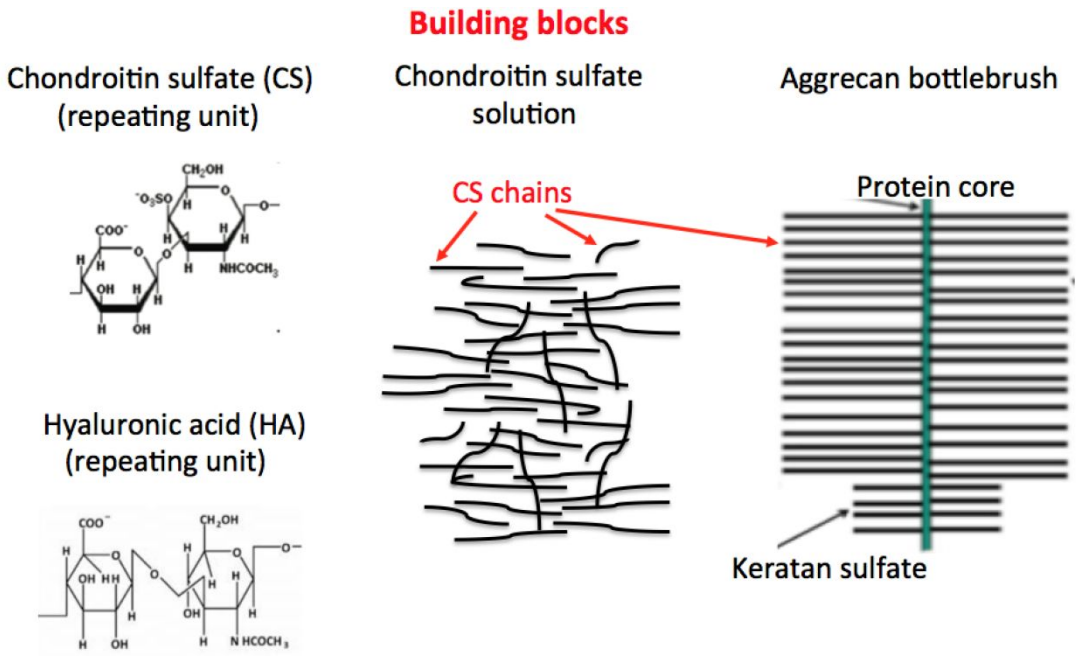

Scheme 1. Main polymeric components of cartilage matrix.

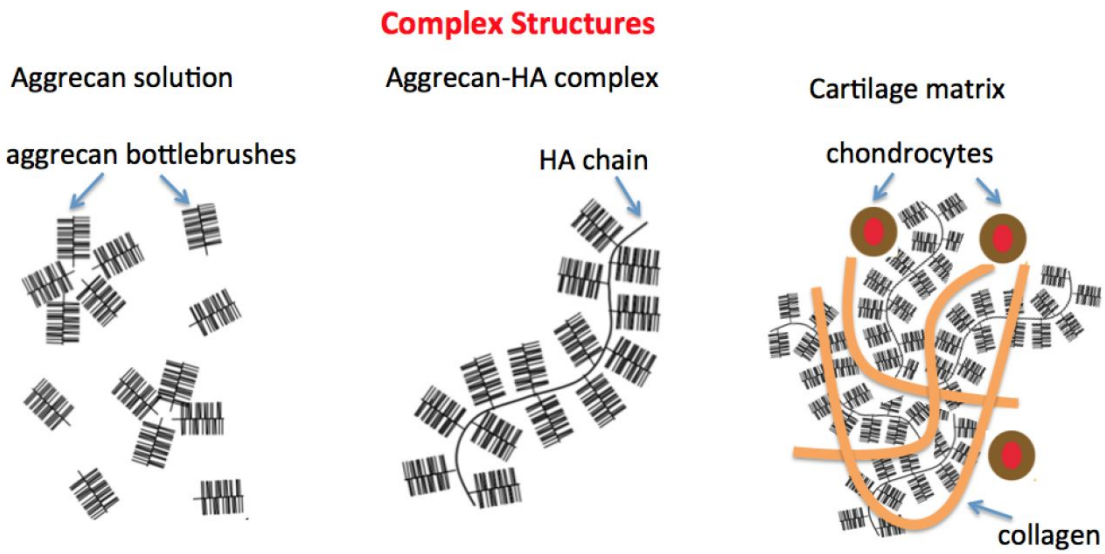

Scheme 2. Structural organization of cartilage polymers.

To understand the overall behavior and the role of the components, it is necessary first to determine the individual properties of each of them. This will serve as a baseline to analyze the mutual interactions. At the macroscopic level, the osmotic pressure is the quantity that reveals the differences between the constituents and also reflects their interactions.

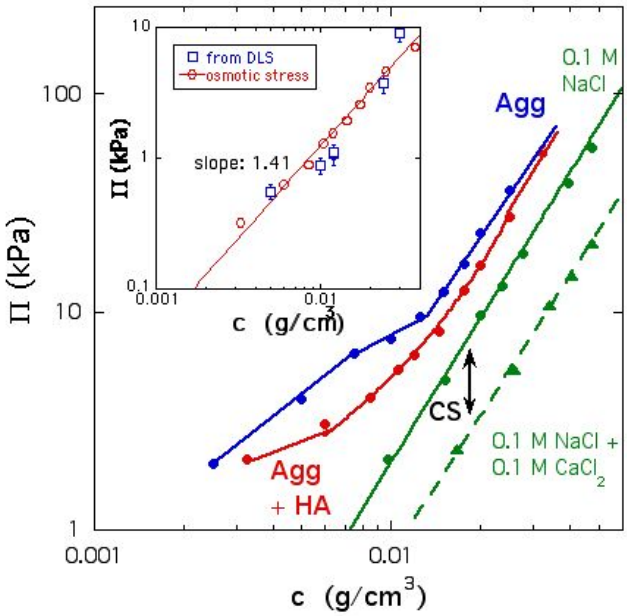

Figure 1. Osmotic pressure Π of solutions of aggrecan (•) and aggrecan-HA complexes (•) in 0.1 M NaCl, compared with CS solutions in 0.1 M NaCl and in 0.1 M NaCl + 0.1 M $CaCl_2$ (continuous and dashed green lines respectively). Curves through the aggrecan and aggrecan+HA data are guides for the eye. Inset shows the variation of Π in collagen in 0.1 M NaCl obtained from osmotic stress experiments and DLS.

Figure 1 shows the dependence of the osmotic pressure Π on the polymer concentration c for solutions of CS, aggrecan and aggrecan-HA complexes in 0.1 M NaCl. In aggrecan and in aggrecan-HA systems Π is greater than in the CS solution in the same concentration range. The osmotic pressure of aggrecan exhibits an inflection around 0.01 g/cm^3, which is associated with self-assembly.[41,42] In the physiological regime (c > 0.02 g/cm^3) the increase of Π is faster for the aggrecan-HA complex, while the slopes for aggrecan and CS solutions do not differ significantly. This similarity suggests that in the aggrecan solution the charged polysaccharide bristles (mainly CS) dominate the interaction with the salt solution, i.e., the role of the protein core is secondary. We note that the osmotic pressure measurements on CS solutions were made in a concentration range that is similar to that of the CS chains (bristles) in the aggrecan bottlebrush (see Scheme 1). The resistance of tissue to osmotic compression requires simultaneously a high value and a strong concentration dependence of the osmotic pressure. The data of Figure 1 thus show the superiority of the bottlebrush structure over the linear CS molecule.

In the double logarithmic representation of Figure 1, CS exhibits power law dependence with an exponent of about 2.2, both with and without calcium chloride. The corresponding dependence for CS in 0.1 M NaCl + 0.1 M $CaCl_2$ is also shown. This amount of $CaCl_2$, however, reduces Π by a factor of approximately 2. A similar reduction in Π with calcium ions has been reported for aggrecan solutions.[40] Calcium ion concentrations of this magnitude, which are much greater than those found physiologically, lead to phase separation in other biopolymers, such as DNA. The stability shown by cartilage proteoglycans in the presence of higher valence ions is a precondition for their role in bone mineralization processes.

In cartilage, the proteoglycan assemblies are embedded in a network of rigid collagen fibers. Under the tensile stress imposed by the swelling of the microgels the collagen is prestressed with the pressure exerted by the aggrecan-HA complex being balanced by tensile stress of the collagen network. The osmotic pressure of the collagen solutions, shown separately in the inset of Figure 1, also displays a power law dependence on the concentration, $\Pi \propto c^m$, where the value of m = 1.57.

Π is about an order of magnitude smaller than for CS. The low value of Π and its weak concentration dependence indicate that the contribution of collagen to the osmotic force in cartilage is small, albeit not negligible. This finding is consistent with previous observations.[12]

To determine the length scale dependence of the arrangement of the proteoglycan molecules in solution, small angle neutron scattering measurements were made on CS and aggrecan in 0.1 M NaCl. Static light scattering measurements were also made on aggrecan-HA solutions. The concentration dependence of the SANS profiles yields information about the extent of overlap among the polymer chains in the solution. In systems where the scattering centers are distinct, the intensity $I(q)$ is proportional to the polymer concentration c. In the absence of overlap, the intensity normalized by the concentration, $I(q)/c$, should therefore be independent of concentration, and the curves for the different concentrations should coincide. In overlapping polymer systems, this behavior is expected at short length scales, i.e., when the resolution of the experiment is high enough to distinguish individual chain sections.

Figures 2a and b show the SANS response of solutions of chondroitin sulfate and aggrecan, respectively. To model the crowded conditions inside the aggrecan bottlebrush, the concentration of the CS solutions was varied in the range 5 – 20% w/w. Since it is known that the GAG chains possess a linear structure due to the semi-rigid character of the polysaccharide backbone, the scattered intensity is expected at high q to display a power law behavior of the form

$$I(q) \propto q^{-1} \tag{5}$$

To highlight the length scale range in which this behavior prevails, the SANS data are presented in the form $qI(q)/c$ vs q. In this representation $qI(q)/c$ is a constant at high q, confirming the rod-like nature at short length scales both of the CS chain and of the GAG bristles in the aggrecan bottlebrush. At lower values of q, these solutions show an upturn due to the large, quasi-static domains that are typical in semi-dilute polyelectrolyte solutions.[56] It is known that the contribution of these clusters to the osmotic pressure of the solution is negligible. In Figures 2a and b the extent of overlap of the molecules in the CS and aggrecan solutions is compared. In CS, for $q > 0.02$, $qI(q)/c$ is a decreasing function of c, i.e., the CS molecules effectively overlap with their neighbors. This is the signature of coupling between the chain segments, even at the resolution of the repeating unit. In contrast to the CS solution, in aggrecan, the curves $qI(q)/c$ coincide over the

entire *q* range, indicating that the aggrecan bottlebrushes are independent and do not interpenetrate. This finding is consistent with the results of molecular dynamic simulations.[39] Absence of interpenetration simultaneously favors resistance to compressive stress (cushioning) as well as low sliding friction.

In the inset of Figures 2a and b, the SANS signals from solutions containing 0.1 M NaCl (crosses) are compared with those with 0.1 M NaCl + 0.1 M $CaCl_2$ (open circles). In both systems the effect of added calcium chloride is small and comparable with the noise.

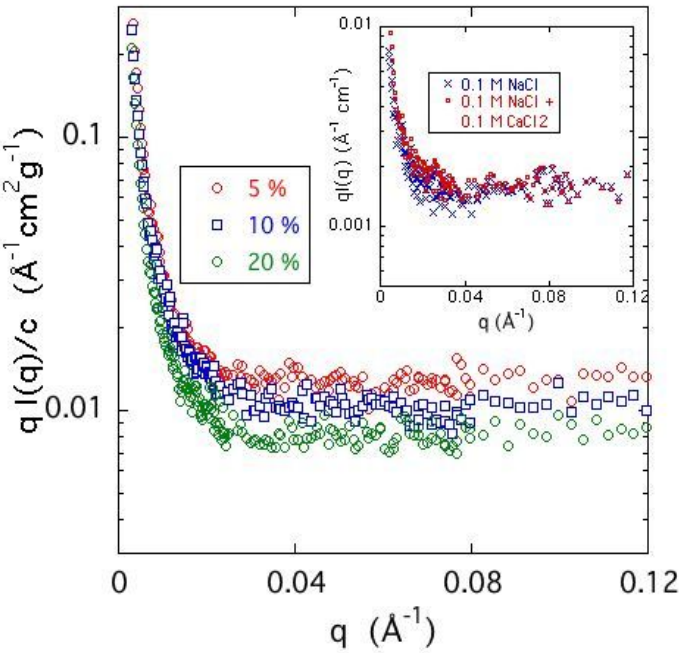

Figure 2a. Plot of $q\,I(q)/c$ *vs* q of CS solutions in 0.1 M NaCl at concentrations c = 5% w/w, 10 % w/w and 20% w/w, inset: plot of $qI(q)$ *vs* q of SANS intensity of 20% w/w chondroitin sulfate solutions in 0.1 M NaCl (×), and in 0.1 M NaCl+0.1 M $CaCl_2$ (O);

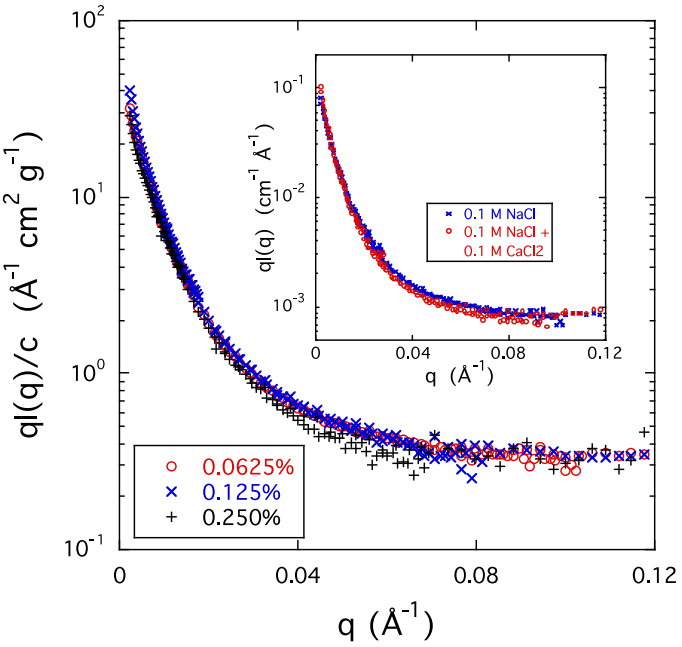

Figure 2b. Plot of $qI(q)/c$ *vs* q for aggrecan solutions in 0.1 M NaCl at concentrations c = 0.0625% w/w, 0.125% w/w and 0.25% w/w, inset: plot of $qI(q)$ *vs* q of SANS intensity of 0.25% w/w aggrecan solutions in 0.1 M NaCl (×), and in 0.1 M NaCl+0.1 M $CaCl_2$ (O).

In cartilage, aggrecan forms complexes with hyaluronic acid, the size of which lies outside the resolution window of the SANS experiment. To visualize the basic structural features of the aggrecan-HA complex, integrated light scattering measurements were made on solutions of aggrecan-HA complexes made at molar ratio 100:1 (Figure 3). For clarity, these results are shown in the Kratky representation $q^2I(q)$ *vs* q, and compared with the corresponding mixture of the two components before complexation. In this representation, the uncomplexed aggrecan + HA mixture shows that, at short times (i.e., before complex formation occurs) the scattering response is dominated by HA, free aggrecan plus aggrecan microgels with branched internal structure, which display the same power law dependence of the intensity as in SANS, i.e., $I(q) \sim q^{-2}$, extending to still lower values of q (open symbols of Figure 3). After complexation, however, the aggrecan molecules self-assemble into the second-order bottlebrush superstructure, which consists of individual aggrecan molecules attached along the central hyaluronic acid filament. The resulting scattering pattern (filled symbols) displays oscillations that are characteristic of worm-like aggregates. In this figure, the geometry of the aggrecan-HA complex is approximated by a solid cylinder of radius 3250 Å (continuous line).

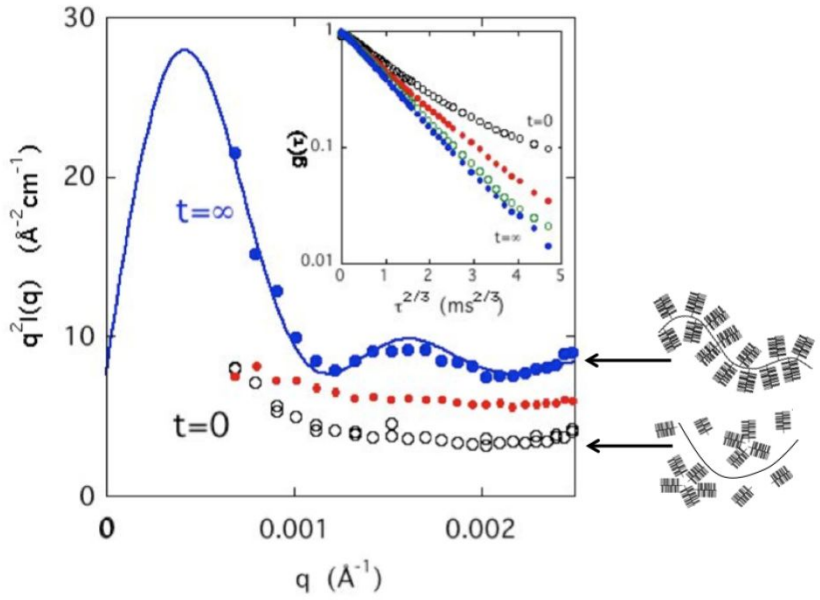

Figure 3. Scattered light intensity from a 0.6% w/w solution of aggrecan containing 1/100 by weight HA (Kratky representation); (o): freshly prepared mixture; (•): mixture after 10 hours. (•): same solution after 48 hours. A continuous curve through the data is the fit to the expression for a cylinder, $(1/q)[J_1(qR)/R]^2$, where $J_1(x)$ is the cylindrical Bessel function of the first kind of order 1, with $R = 3250$ Å. This figure, however, which covers a q range well below that explored by SANS in Fig. 2, displays an additional almost flat response of the signal due to random assemblies from the freshly prepared mixture, in which $I(q) \propto q^{-2}$.

To monitor the progress of complexation, DLS measurements were made on the aggrecan-hyaluronic acid mixture as a function of time. The inset of Figure 3 shows the change in the field correlation function $g(\tau)$ at different stages of complexation. As noted in the experimental section $g(\tau)$ adopts the stretched exponential form

$$g(\tau) = \exp[-(\Gamma\tau)^p] \qquad (6)$$

where the exponent p tends to the value 2/3 in the complexes. The complex formation was considered to be complete when no further change was detected in the plot of $\log[g(\tau)]$ vs $\tau^{2/3}$. It is notable that the aggrecan-HA complexes, which form spontaneously even in the absence of link protein, remain stable for several days.

Loading biological tissues is generally accompanied by changes in shape and swelling. The deformability and cushioning efficiency of cartilage are governed by the osmotic properties and the underlying molecular architecture. The rate of return of the volume from the deswollen

condition to the initial state, however, is controlled by the relaxation time of the polymer network. This process involves mutual exchange between the polymer segments and the surrounding fluid medium (ions, water molecules). The rate of exchange is quantified by the collective diffusion coefficient D, which determines the frequency at which repetitive tasks can be pursued without damage to the tissue. Fast and full recovery requires high values of D.

To compare the relaxation rates Γ of the proteoglycan systems, DLS measurements were performed. In Figure 4 typical correlation functions $g(\tau)$, measured at $\theta = 90°$, are shown for solutions of CS, aggrecan and aggrecan-HA complexes. For the CS solution, $g(\tau)$ displays two characteristic relaxation processes, separated by approximately two orders of magnitude in time τ, while for the aggrecan containing systems only one relaxation mechanism is observed. The relaxation rate of the fast process in CS varies as q^2, as shown in the inset of **Figure 5** (upper data set) and a slow component, which varies as q^3. The slow mode is the relaxation response of the large clusters in the solution that cause the low q upturn in the SANS response (Fig 2a). The q^2 dependence of the fast mode implies that it is diffusive. This process controls the kinetics of swelling. Its relaxation rate is substantially greater than that of aqueous solutions of neutral polymers,[52,57] which is beneficial to the function of rapid tissue hydration.

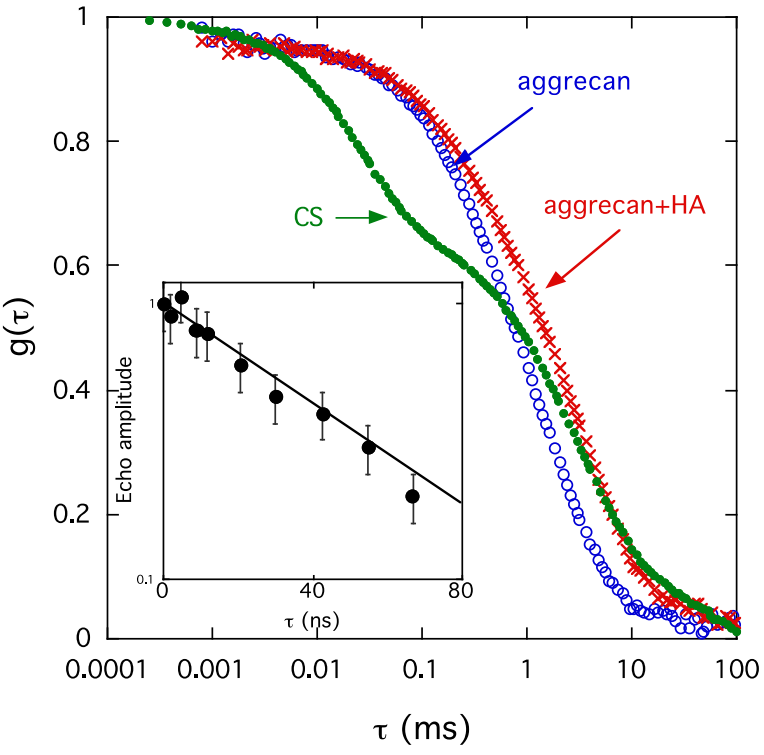

Figure 4. DLS field correlation function $g(\tau)$ from solutions containing 0.1 M NaCl with 2% w/w CS (•), with 0.6% w/w aggrecan (o), and with aggrecan + hyaluronic acid in 100:1 ratio (×). Inset: NSE decay at $q = 0.087$ Å^{-1} for the aggrecan solution.

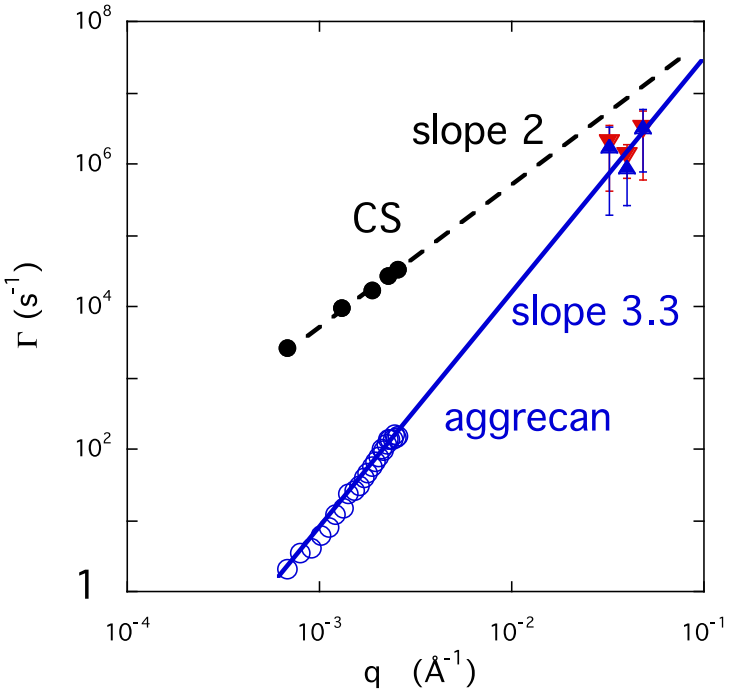

Figure 5. Relaxation rate Γ as a function of q for chondroitin sulfate (•) and aggrecan (o) solutions measured by DLS. The data points at $q > 10^{-2}$ Å^{-1} are neutron spin echo measurements from aggrecan solutions.

To quantify the osmotic recovery rate in the CS solution we derive the collective diffusion coefficient D from the fast component of the DLS correlation function. Figure 6 shows the concentration dependence of D for CS solutions containing 0.1 M NaCl (filled symbols). The continuous line through the data points is the power law fit

$$D = 6.2\ 10^{-6}\ c^{0.42}\ \text{cm}^2\text{s}^{-1} \qquad (7)$$

Addition of calcium chloride reduces the value of D. In a 10% w/w solution of CS with 0.1 M NaCl, D decreases smoothly from 2.6 10^{-6} cm^{2}s^{-1} to 1.1 10^{-6} cm^{2}s^{-1} at 0.2 M $CaCl_2$ (open circles).

In this system, well beyond physiological concentrations of $CaCl_2$, D still remains greater than in neutral polymers.

Unlike suspensions of particles of hydrodynamic radius R_H, or solutions of linear polymers such as CS, in which a well defined hydrodynamic correlation length can be measured, in crowded aggrecan solutions no particular hydrodynamic length prevails. In this case the apparent diffusion coefficient is determined only by the length scale of the measurement, $1/q$, with the result that the relaxation rate Γ becomes proportional to q^3.[55] The relaxation response of the aggrecan solution (Figure 5) exhibits only q^3 behavior, resembling the slow mode of CS. Neutron spin echo measurements, shown in Figure 5, indicate that at high q (≈ 0.1 Å^{-1}), Γ of the aggrecan solution approaches that of CS. The absence of q^2 dependence in the aggrecan brings independent confirmation of the lack of interpenetration of the bottlebrush bristles. Complexation with hyaluronic acid slightly slows down the dynamics of the aggrecan aggregates (Fig. 4).

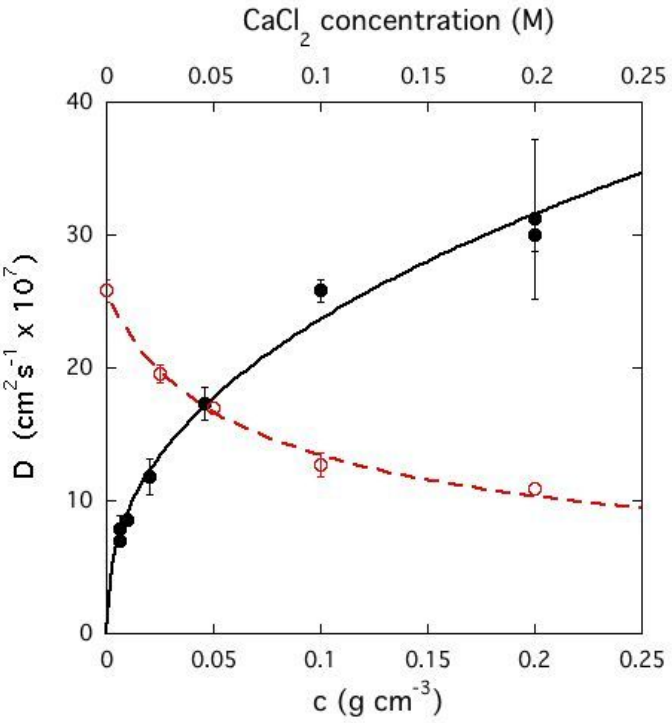

Figure 6. Filled symbols, lower scale: dependence of D on polymer concentration c in solutions of CS in 0.1 M NaCl; open symbols, upper scale: variation of D as a function of $CaCl_2$ concentration (c_{Ca}) with 0.1 M NaCl, with CS concentration 0.1 g cm^{-3}.

The q^3 behavior is characteristic of microgels. In the aggrecan-HA system it is the microgel structure that provides enhanced mechanical stability and reversible shape recovery. The microgel architecture of aggrecan is particularly favorable for lubrication. An attribute of microgels is that under compressive stress they release liquid, thus contributing to the low friction lubrication properties of the cartilage.[58] Owing to its crowded bristle structure the local concentration of the highly charged GAG chains is elevated, which enhances the intrinsic stiffness of the molecule. This stiffness, which prevents interpenetration and limits entanglement formation, further reduces friction between neighboring bottlebrushes and favors mutual alignment.

It is noteworthy that the behavior of proteoglycan solutions is substantially different from that of typical polyelectrolytes, for which the dynamic properties are highly sensitive to multivalent ions, and undergo phase separation. In solutions of CS or of aggrecan (fig 5 and fig 4 inset respectively), however, neither the dynamic properties nor the structure display signs of instability even at high calcium ion concentration. These findings indicate that the main effect of calcium ions is to modify the average thermodynamic interactions between the CS molecules. They affect the relaxation rate but, as confirmed by SANS (Fig 2a), they induce no permanent structural changes. Insensitivity to calcium ions is a prerequisite for these systems to function biologically in the bone mineralization process.

Biomechanical Implications

In this section we summarize the main results in terms of the load bearing properties of cartilage. The load bearing resistance of proteoglycan assemblies is evaluated from the concentration dependence of the osmotic pressure Π, from which the osmotic modulus $\kappa = c\partial\Pi/\partial c$ can be derived. Figure 7 shows the variation of κ for the three proteoglycan systems, as well as for the collagen solution. The osmotic modulus is the highest in the aggrecan-HA complex, and increases faster than in the pure aggrecan solution with concentration. This implies that the creation of a secondary bottlebrush structure not only reinforces the mechanical stability of these proteoglycan assemblies but also enhances their osmotic resistance. The osmotic modulus of the aggrecan is greater than that of the CS solution. Since the bristles of the aggrecan molecules consist of GAG chains, it is reasonable to assume that the higher osmotic modulus of aggrecan is the consequence of its bottlebrush structure.

Aggrecan and its complexes with HA form microgels, even at concentrations well below the physiological range. The small size and dispersed character of the microgel particles ensure rapid response to sudden changes in external loads, e.g., in shock absorption. The absence of interpenetration of the bottlebrush bristles enhances the cushioning capacity of the cartilage. It also prevents chain entanglement between bottlebrushes, hence reducing friction. Moreover, under compressive load, microgel particles deswell and release lubricating fluid, further reducing friction in the articulation.

In contrast to proteoglycans, in the collagen solution the value of κ is much smaller and its variation with concentration is substantially weaker, which is consistent with the known limited role of collagen in the load bearing properties of cartilage.

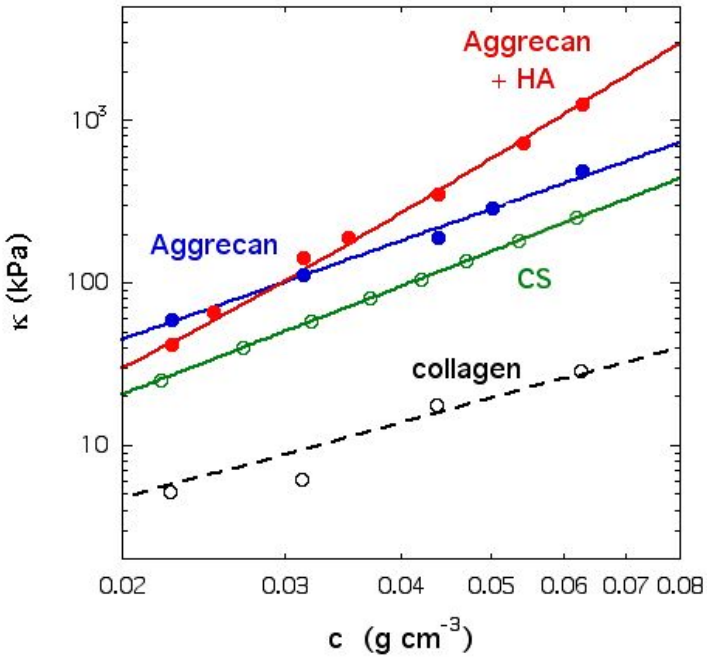

Figure 7. Concentration dependence of the osmotic modulus $\kappa = c\partial\Pi/\partial c$ of solutions of CS, aggrecan, and aggrecan-HA complexes in 0.1 M NaCl, compared with that of collagen.

Fast response of cartilage to external loading requires a high collective diffusion coefficient *D*. CS solutions at near physiological concentrations of NaCl show that *D* is 5 - 10 times greater than in aqueous solutions of typical neutral polymers. In the presence of calcium chloride, *D* is a weakly decreasing function of the calcium ion concentration. For aggrecan and the aggrecan-HA

complexes the dynamic response is dominated by the microgel structure of the large assemblies, which is insensitive to changes in the ionic environment.

An unexpected feature of proteoglycan assemblies is the insensitivity of their structural and dynamic properties to the presence of calcium ions. Over the length scale range explored by SANS, no detectable structural change occurs, even at ionic strengths (0.2 M) much higher than the physiological concentration range. Such stability is a prerequisite for the function of cartilage in its role in bone formation.

To illustrate how each level of structural hierarchy contributes to the biomechanical properties of the proteoglycan assemblies, we summarize the results in terms of ionic resistance, recovery rate and load bearing capacity. Table 1 compares the specific functional features of the different levels of hierarchy of the proteoglycan systems.

Table 1. Comparative response of proteoglycan assemblies at different hierarchical levels.

Function	Stability to ions	Relaxation behavior	Load bearing resistance
CS solution	resistance to ionic environment local rigidity	Solution-like Fast	reference baseline
Aggrecan molecule	large scale rigidity non interpenetration	Microgel-like	enhanced resistance to compressive forces
Aggrecan-HA complex	large scale rigidity non interpenetration	Microgel-like	mechanical stability, large scale integrity

Conclusions

In this study, the roles of the different levels in the hierarchical structure of cartilage proteoglycans are investigated using complementary experimental techniques, including osmotic pressure measurements, neutron scattering and light scattering. The linear hydrophilic charged polysaccharide chondroitin sulfate (CS) is used as a model proteoglycan molecule to identify the basic physical chemical properties (ion sensitivity, dynamic relaxation rate and osmotic compression modulus) that govern the behavior of higher order assemblies. The different levels considered are the linear molecule CS, the bottlebrush shaped aggrecan molecule, the aggrecan-hyaluronic acid complex and, lastly, the collagen matrix. The main functional properties of

cartilage we consider here are the osmotic resistance to external loading, the characteristic deformation and recovery rates of the tissue, and the structural stability in different physiologically relevant ionic environments. This latter is important since cartilage is exposed to calcium ions associated with bone mineralization.

The osmotic modulus determined as a function of the proteoglycan concentration, increases with the molecular architectural complexity following the order CS < aggrecan < aggrecan-HA complex. The hierarchical bottlebrush configuration, which prevents interpenetration among the bristles of the aggrecan bottlebrushes, enhances both the mechanical properties and the osmotic resistance.

The rate of recovery after compressive load is governed by the collective diffusion coefficient. In CS solutions collective diffusion is fast, comparable with that of the GAG chains inside the aggrecan molecule. In CS solutions D is a weakly decreasing function of calcium ion concentration, while in aggrecan and aggrecan-HA complexes, the relaxation rate is practically unaffected by the presence of calcium ions.

ACKNOWLEDGEMENTS

This research was supported by the Intramural Research Program of the NICHD. The authors acknowledge the support of the National Institute of Standard an Technology, U.S. Department of Commerce, for providing access to the NG3 small angle neutron scattering instrument used in this experiment. This material is based upon activities supported by the National Science Foundation under agreement no. DMR-1508249. The authors thank the ILL, Grenoble for beamtime on the IN15 instrument.

Data Availability Statement: The data that support the findings of this study are available from the corresponding author upon reasonable request.

Conflict of Interest: The authors declare no conflict of interest.

References

1. Biology of Proteoglycans (Biology of Extracellular Matrix), T. Wight and R. Mecham eds., Academic, New York, 1987.

2. V. C. Hascall, IS1 Atlas of Science: Biochemistry **1988**, *1*, 189.

3V.C. Mow, W. Zhu and A. Ratcliffe, A. Structure and function of articular cartilage and meniscus, in Basic Orthopedic Biomechanics, eds. V.C. Mow and W.C. Hayes, Raven Press, New York, 1991.

4. C. Won and L.R. Sah, Biomechanics of Articular Cartilage, in An Introductory Text to Bioengineering (Advanced Series in Biomechanics), eds. S. Chien, P.C.Y. Chen and Y.C. Fung, World Scientific Publishing Co. 2008.

5. P. L. Chandran and F. Horkay, Aggrecan, an Unusual Polyelectrolyte: Review of Solution Behavior and Physiological Implications, *Acta Biomater.* 2012, **8**, 3–12.
,*

6. A. Chremos and F. Horkay, Coexistence of Crumpling and Flat Sheet Conformations in Two-Dimensional Polymer Networks: An Understanding of Aggrecan Self-Assembly, *Phys. Rev. Lett.* 2023. **131**, 138101

7. T. Kobayashi, T. Chanmee and N. Itano, Hyaluronan: metabolism and function. Biomolecules 2020. **10**, 1525.

8. A. G. Ogston, (1970) *in* Chemistry and Molecular Biology of the Intracellular Matrix: The Biological Functions of the Glycosaminoglycans (A. B. Andre, Ed.), Vol. 3, 1231–1240, Academic Press, London.

9. A. Maroudas, H. Evans and L. Almeida, Cartilage of the hip joint. Topographical variation of glycosaminoglycan content in normal and fibrillated tissue. *Ann Rheum Dis.* 1973, **32,** 1–9.
10. A. Maroudas and M. Venn, Chemical composition and swelling of normal and osteoarthrotic femoral head cartilage. II. Swelling. *Ann. Rheum. Dis.* 1977, **6**, 399– 406.

11. A. Maroudas, Balance between swelling pressure and collagen tension in normal and degenerate cartilage, *Nature* 1976, **260**, 808–809.

12. P. J. Basser, R. Schneiderman, R. A. Bank, E. Wachtel and A. Maroudas, Mechanical properties of the collagen network in human articular cartilage as measured by osmotic stress technique. Archives of Biochemistry and Biophysics, 1998, **351**, 207-219.

13. H. Shinar and G.Navon, Multinuclear NMR and microscopic MRI studies of the articular cartilage nanostructure. *NMR Biomed*, 2006, **19**, 877– 893.

14. W. R. T. Witschey, A. Borthakur, M. Fenty, B.J. Kneeland, J.H. Lonner, E.L. McArdle, M. Sochor and R. Reddy, R. $T_1\rho$ MRI quantification of arthroscopically confirmed cartilage degeneration, *Magn. Reson. Med.* 2010, **63**, 1376– 1382.

15. A. Borthakur, E. Mellon, S. Niyogi, W. Witschey, J.B. Kneeland and R. Reddy, Sodium and T1rho MRI for molecular and diagnostic imaging of articular cartilage. *NMR Biomed.* 2006, **19**, 781– 821.

16. R. Reddy, E.K. Insko, E. A. Noyszewski, R. Dandora, J.B.Kneeland and J.S. Leigh, Sodium MRI of human articular cartilage in vivo. *Magn. Reson. Med.* 1998, **39**, 697– 701.

17. E.M. Shapiro, A. Borthakur, J,H. Kaufman, J.S. Leigh and R. Reddy, Water distribution patterns inside bovine articular cartilage as visualized by ^{1}H magnetic resonance imaging. *Osteoarthritis Cartilage* 2001, **9**, 533– 538.

18. J. Xu, P. Zhu, M. D. Morris, A. Ramamoorthy, Solid-state NMR spectroscopy provides atomic-level insights into the dehydration of cartilage. *J. Phys. Chem. B*, 2011, **115**, 9948–9954.

19. N.P. Camacho, P. West, P.A. Torzilli, R. Mendelsohn, FTIR microscopic imaging of collagen and proteoglycan in bovine cartilage. Biopolymers, 2001, 62, 1-8. A

20. A. Boskey and N. P. Camacho: FT-IR Imaging of Native and Tissue-Engineered Bone and Cartilage, Biomaterials. 2007, **28**, 2465–2478.

21. P.A. West, M.P. Bostrom, P.A. Torzilli, and N.P. Camacho, Fourier transform infrared spectral analysis of degenerative cartilage: an infrared fiber optic probe and imaging study. *Appl Spectrosc.* 2004, **58**, 376–381.

22. L.M. Miller and P. Dumas, P.: Chemical imaging of biological tissue with synchrotron infrared light. *Biochim Biophys Acta.* 2006, **1758**, 846–857.

23. S. S. Stivala, A. Patel, B. Khorramian, J. D. Gregory, S. Damle: Small-angle x-ray scattering of bovine nasal cartilage proteoglycan in solution. Biopolymers, **26**, 633–650 (1987).

24. J. Mollenhauer, M. Aurich, C. Muehleman, G. Khelashvilli and T. C. Irving: X-Ray Diffraction of the Molecular Substructure of Human Articular Cartilage, *Connective Tissue Research*, 2003, **44**, 201–207.

25. A. Naito, S. Tuzi and H. Saito, HA high-resolution 15N solid-state NMR study of collagen and related polypeptides. The effect of hydration on formation of interchain hydrogen bonds as the primary source of stability of the collagen-type triple helix. Eur J Biochem. 1994, **224**, 729-34.

26. D. Huster, J. Schiller and K. Arnold: Dynamics of collagen in articular cartilage studied by solid-state NMR methods, *Methods in Molecular Medicine*, 2004,**101**, 303-318.

27. R. K. Rai and N. Sinha, Dehydration-Induced Structural Changes in the Collagen–Hydroxyapatite Interface in Bone by High-Resolution Solid-State NMR Spectroscopy, *J. Phys. Chem. C*, 2011, **115**, 14219–14227.

28. R. Ellis, E. Green and C. P. Winlove, Structural analysis of glycosaminoglycans and proteoglycans by means of Raman microspectrometry, *Connect. Tissue Res.* 2009, **50**, 29–36 .

29. A. Bonifacio and V. Sergo, Effects of sample orientation in Raman microspectroscopy of collagen fibers and their impact on the interpretation of the amide III band, *Vibrat. Spectrosc.* 2010, **53**, 314–317 .

30. K. A. Dehring, A. R. Smukler, B. J. Roessler and M. D. Morris, Correlating changes in collagen secondary structure with aging and defective type II collagen by Raman spectroscopy, *Appl. Spectrosc.* 2006, **60**, 366–372 .

31. H. Saito and M. Yokoi: A 13C NMR study on collagens in the solid state: hydration/dehydration-induced conformational change of collagen and detection of internal motions. *Journal of Biochemistry*, 1992, **111**, 376-382.

32. D. Reichert, O. Pascui, E. R. DeAzevedo, T. J. Bonagamba, K. Arnold and D. Huster, A solid-state NMR study of the fast and slow dynamics of collagen fibrils at varying hydration levels. *Magnetic resonance in chemistry*, 2004, **42**, 276-284.

33. D. Dean, L. Han, C. Ortiz and A. J. Grodzinsky, Nanoscale conformation and compressibility of cartilage aggrecan using microcontact printing and atomic force microscopy. *Macromolecules* 2005. **38**, 4047-4049.

34. D. Dean, L. Han, A.J. Grodzinsky and C. Ortiz, Compressive nanomechanics of opposing aggrecan macromolecules, *J.Biomech*. 2006, **39**, 2555-2565.

35. A. Chremos, J.F. Douglas, P.J. Basser and F.Horkay, Prestressed Composite Polymer Gels as a Model of the Extracellular-Matrix of Cartilage, *Gels* 2022, **8**, 707.

36. A. Chremos, J, F. Douglas, P. J. Basser and F. Horkay, Molecular dynamics study of the swelling and osmotic properties of compact nanogel particles, *Soft Matter* 2022, **18**, 5278-6290.

37. F.Horkay, A. Chremos, J.F. Douglas, R.L. Jones, J. Lou and Y.Xia, Systematic investigation of synthetic polyelectrolyte bottlebrush solutions by neutron and dynamic light scattering, osmometry, and molecular dynamics simulation, *J. Chem. Phys.* 2020, **152**, 194904

38. F. Horkay, A. Chremos, J.F. Douglas, R.L. Jones, J. Lou and Y.Xia. Comparative experimental and computational study of synthetic and natural bottlebrush polyelectrolyte solutions. *J. Chem. Phys.* 2021, **155**, 074901.

39. R. J. Nap and I. Szleifer: Structure and Interactions of Aggrecans: StatisticalThermodynamic Approach, *Biophysical Journal,* 2008, **95**, 4570–4583.

40. F. Horkay, P.J. Basser, A.-M. Hecht and E. Geissler, Insensitivity to Salt of Assembly of a Rigid Biopolymer Aggrecan. *Phys. Rev. Lett*. 2008. **101**, 068301.

41. F. Horkay, P.J. Basser, A.-M. Hecht and E. Geissler, Gel-like Behavior in Aggrecan Assemblies J. Chem. Phys. 2008, **128**, 135103.

42. F. Horkay, J.F. Douglas and S. R. Raghavan, Rheological Properties of Cartilage Glycosaminoglycans and Proteoglycans, *Macromolecules* 2021, **54**, 5, 2316–2324

43. K. Li, C. Zhang, L. Qiu, L. Gao and X. Zhang, Advances in application of mechanical stimuli in bioreactors for cartilage tissue engineering. *Tissue Eng Part B Rev* 2017, **23**, 399–411.

44. T. Stampoultzis, P. Karami and D. P. Pioletti, Thoughts on cartilage tissue engineering: a 21st century perspective. *Curr Res Transl Med* 2021, **69**, 103299

45. F. Horkay and M. Zrinyi, Studies on Mechanical and Swelling Behavior of Polymer Networks Based on the Scaling Concept, 4. Extension of the Scaling Approach for Gels Swollen to Equilibrium in a Diluent of Arbitrary Activity. *Macromolecules* 1982, **15**, 1306-1310.

46. F. Horkay and J.F. Douglas, Evidence of Many-Body Interactions in the Virial Coefficients of Polyelectrolyte Gels, *Gels* 2022, *8*(2), 96-108.

47. F. Horkay, P.J. Basser and E. Geissler, Ion-induced changes in DNA gels, Soft Matter 2023, 19, 5405-5415.

48. H. Vink, Precision measurements of osmotic pressure in concentrated polymer solutions. *Eur. Polym. J.* 1971, *7*, 1411–1419.

49. J.S. Higgins and H.C. Benoit, Polymers and Neutron Scattering, Clarendon Press-Oxford (1994).

50. O. Glatter and O. Kratky, Small Angle X-Ray Scattering, Academic Press (1982)

51. NIST Cold Neutron Research Facility, NG3 and NG7 30 m SANS Instruments Data Acquisition Manual. 2002. Available online: https://www.nist.gov/ncnr/ng7-sans-small-angle-neutron-scattering.

52. F. Horkay, W. Burchard, E. Geissler and A.M. Hecht, Thermodynamic Properties of Poly(vinyl alcohol) and Poly(vinyl alcohol-vinyl acetate) Hydrogels. *Macromolecules* 1993, **26,** 1296-1303.

53. P. Berne and R. Pecora, *Dynamic Light Scattering*, Academic Press, London, 1976.

54. M. B. Huglin, Ed., *Light scattering from polymer solutions*, Academic Press Inc., London, 1972.

55. P.G. de Gennes *Scaling Concepts in Polymer Physics*, Cornell, Ithaca 1979.

56. M. Drifford and J.P. Dalbiez, Effect of salt on sodium polystyrene sulfonate measured by light scattering. *Biopolymers* 1985, **24**, 1501-1514.

57. A.M. Hecht and E. Geissler, Dynamic light scattering from polyacrylamide-water gels. *J. Physique* 1978, **39,** 631-638.

58. E. D Bonnevie and L.J. Bonassar, A century of cartilage tribology research is informing lubrication therapies. *J. Biomech. Eng*. 2020, **142**, 031004.